INVESTIGATION OF ONE-SIDED RADIATION-BASED APPROACHES TO DETECTION OF VISUALLY OBSCURED THREATS

William R. Scott
University of Ontario Institute of Technology, Oshawa, ON
william.scott2@mycampus.uoit.ca

ABSTRACT

In an effort to detect visually obscured objects, a number of different techniques are employed. One such technique is called Coded Aperture Imaging (CAI). Coded apertures operate with no lenses, meaning there is an infinite depth of field, the image does not suffer from chromatic aberration and images can be formed from sources other than visible light, such as high energy radiation. When gamma radiation is projected at an object it will produce a detector response which can be reconstructed to reveal the original object.

Computer modeling was performed using a specific binary matrix to generate a three-dimensional mask, using holes for zeros and tungsten for ones. Radiation transport software called MCNPX was used to simulate radiation passing through the holes and registering on the detector. Due to the number of holes, the projection is convoluted, with many copies of the image blurred together. Digital reconstruction techniques were implemented using MATLAB, involving mathematical manipulation in the frequency domain.

Since gamma rays are affected by the material density, images consist of shades of grey, resembling medical x-rays. Presently, we can image with transmission x-rays, however, the goal is to image the backscatter from an object which would permit imaging of concealed objects.

1 INTRODUCTION

Digital cameras are becoming a very common and important device in today's society; with many modern cell phones also containing this feature. The principle behind digital cameras has evolved very quickly; however, they are still limited to the properties of visible light. Since light waves cannot bend around corners or travel through walls, digital cameras cannot take pictures of these hidden objects. This presents a challenge because there are many cases where this ability would be helpful, such as scanning vehicles at border crossings, helping police recover evidence, finding humans trapped in collapsed buildings, discovering hidden hostages, searching for cracks in concrete or pipes and imaging features in places where human access is very limited, such as the reactor building in a nuclear plant. In order to address these challenges, a number of one-sided imaging techniques are typically used. Millimetre waves, ultrasound, radar, x-ray fluorescence and Coded Aperture Imaging (CAI) are some examples. The focus of this research was CAI.

CAI began as a means of improving x-ray imaging of distant stars and has now, with the increase in computer processor power, become a feasible technique for imaging near-field objects on Earth. The imaging of stars was possible first because at very large distances, the incoming rays are essentially parallel [1], so they produce a projection through the aperture with minimal scattering. In the more recent near-field applications, because the source is much closer to the aperture, the rays scatter through each hole in the aperture, creating a convoluted image. This convolution is composed of a faint image from each hole in the aperture, all blurred together. The reason for using a coded aperture is that each faint image can be associated with the hole it came from, providing the aperture and decoding aperture are carefully chosen. This is the main principle behind coded apertures. Using a computer to perform the calculations, a convoluted projection can be reconstructed to reveal the original image.

2 APERTURE THEORY

Prior to discussing coded aperture theory, an overview of simple apertures is required. The pinhole camera is a classic example of the application of a single-hole aperture. Early photographs were produced by a box, sealed at the edges, with a single pinhole in the centre of one side. The light would enter the box through the tiny hole and the image would appear on the film on the far side of the box, inverted. The image is inverted because of the path of the light rays, as shown in the following diagram, Figure 1.

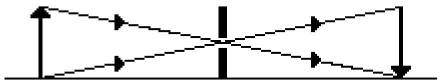

Figure 1: Pinhole ray diagram

Although this single aperture process is simple; the pinhole only allows a small amount of light to enter, producing a very faint image.

In order to produce a recognizable image, the amount of light reaching the film must be increased. Increasing the exposure time will improve light intensity, provided the subject does not move. Any movement will blur the image. A larger pinhole will improve light intensity by allowing more light in a given time, but at the cost of image resolution. A unique property of the pinhole camera is that the size of the pinhole dictates the size of the smallest element which can be resolved. This means that a larger pinhole will produce a brighter image, with lower resolution.

To solve this problem, photographers began using lenses to focus more light onto the film, producing brighter and clearer images. This works well for visible light, but high energy radiation is not affected by lenses. In order to image concealed objects, high energy radiation is required, and so is the ability to focus it.

If a larger pinhole will not produce the desired resolution and lenses have no effect on focusing x-rays, the other way to increase the light intensity is with multiple pinholes, which is the essence of coded apertures. The light intensity is increased not by larger holes, but by many small ones.

If the multiple pinholes are arranged in a systematic way, they will produce an image which is convoluted. One faint image from each pinhole is generated and all are projected on top of each other, which makes what appears to be a blurred non-descript pattern. The key factor to coded aperture imaging is in the aperture mask design. In all cases the aperture is accompanied by a complementary decoding aperture which is used in conjunction with the detector response to reconstruct the image.

The image convolution poses the greatest challenge for CAI, although coded apertures have a number of advantages over traditional lenses. First, unlike the lenses in modern cameras, coded apertures do not suffer from chromatic aberration. In a camera lens, different wavelengths of light bend at different angles, so the camera requires a second lens to correct for this phenomenon, while coded apertures have no such requirement. Where camera lenses have a focal length based on their curvature, coded apertures do not. In fact they have an infinite depth of field. Both of these factors allow pinhole cameras to produce images from sources other than visible light, such as the high energy radiation of x-rays and gamma rays.

Where traditional cameras use film to collect the light and produce the image, a photon detector is used in CAI. The photon detector has the same number of elements as the aperture, 79x79 in this case, and it is positioned so it maximizes the number of photons registered. A simple and effective aperture design is a Modified Uniformly Redundant Array, or MURA [2]. Each aperture has a corresponding decoding aperture, differing only by the centre element, which should sufficiently restore the image quality to recognize the original object. In the case of MURAs, the apertures are square and have a unique property that their anti-mask aperture, the exact opposite, is a 90 degree rotation of the original aperture. This makes mask fabrication easier, as only one requires machining. Depending on the thickness of the mask, a backing, transparent to x-rays, may be required to support the tungsten elements. There are many conditions and restrictions governing these MURAs, which will be discussed in the mathematics section.

3 MATHEMATICS

The complex mathematics of CAI can be broken down into small steps with fewer complexities. The first discussion is of aperture generation. There are many types of apertures, each having strengths and weaknesses geared to different applications. In the case of MURAs the side length must be a prime number so there is a defined centre element. This represents the single pinhole in the mathematics. When referring to the matrices, A1 is the mask aperture and A2 is the anti-mask aperture, likewise with the decoding apertures G1 and G2. The process of mathematically generating MURAs is given by Equations 1 and 2 [3]:

$$A_{ij} = \begin{cases} 0 \quad \text{if } i = 0 \\ 1 \quad \text{if } j = 0, i \neq 0 \\ 1 \quad \text{if } c(i)c(j) = 1 \\ 0 \quad \text{otherwise} \end{cases} \tag{1}$$

$$G_{ij} = \begin{cases} 1 \text{ if } i \oplus j = 0 \\ 1 \text{ if } A_{ij} = 1, i \oplus j \neq 0 \\ 0 \text{ if } A_{ij} = 0, i \oplus j \neq 0 \end{cases} \tag{2}$$

Where:
$\oplus$ is a periodic summation, meaning the modulus of i and j (the remainder after division) or
$i \oplus j$ = i mod j
and c(i) , c(j) are quadratic residues [4].

This matrix arrangement is not the working configuration, but is a simple way to generate the pattern based on matrix indices. In order for this to become a MURA, the entire set of data must be cyclically shifted so the first element (0,0) is moved to the centre of the matrix, (39,39) in the case of a 79x79 matrix [5].

The A1 aperture is the exact opposite of A2, meaning each 0 becomes 1 and each 1 becomes 0, where 0 is white and 1 is black, as shown in Figures 2 and 3 respectively. G1 is identical to A1 with the exception of the centre element which is switched, the same goes for A2 and G2; where G1 is shown in Figure 4 and G2 in Figure 5.

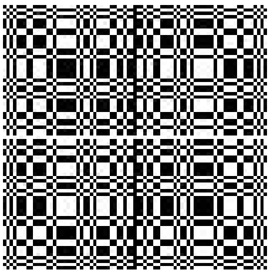

Figure 2: A1 aperture

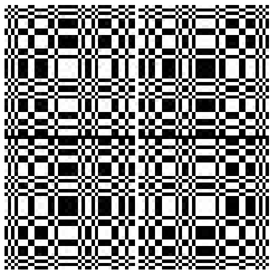

Figure 3: A2 aperture

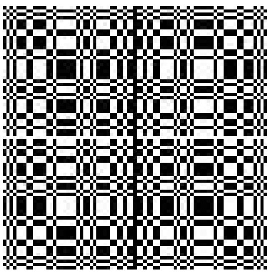

Figure 4: G1 aperture

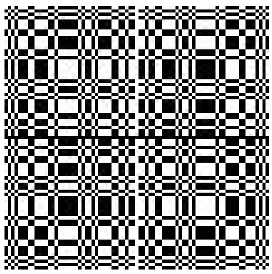

Figure 5: G2 aperture

Image reconstruction is summarized by Equation 3 [3]:

$$\hat{S}_{ij} = \sum_k \sum_l D_{ij} G_{i \oplus k, j \oplus l} \tag{3}$$

$\hat{S}_{ij}$ indicates the result is in frequency space after a Fourier transform (FT). So the FT of D, the detector response, and G, the decoding aperture are multiplied together when the mod conditions are satisfied. Inspection of the mod conditions reveals that since i=j=k=l= side length (in this case 79) a single element in the reconstruction is composed of contributions from every element in the detector response, correlated with the decoding aperture in a diagonal pattern. This is the most computationally intensive part, making the number of calculations 2*(side length)^4. This result must then be inverse Fourier transformed to return the values to the spatial domain, in order to see the image. The purpose of the Fourier transforms is to smooth out the rigid step data into a function of sine and cosines and allow the multiplication of D and G to produce a wave interaction operation compared to binary multiplication. The zero values in G must be smoothed out or they will ruin the reconstruction, by cancelling out valid data. Once all the elements are present, this is a very logical method of image reconstruction.

The other important aspect of MURAs is the ability to use a mask and anti-mask in conjunction, to image more clearly. This allows a normal run with a mask, and a second run with an anti-mask, which is just the opposite of the mask, (1 becomes 0, 0 becomes 1). The purpose is to cancel artefacts which arise due to the nature of the MURA pattern and are unwanted, while at the same time, reinforcing the image itself. The two reconstructions are summed together in the spatial domain and the results of this are much clearer compared to either image on its own.

4 COMPUTER SOFTWARE

In order to model the transport of radiation and it's interaction with the apertures, a computer simulation was done. The radiation simulation was done in Monte Carlo Neutral Particle with eXtended features, or MCNPX [6]. The image reconstruction mathematics were performed in MATLAB [7]. The whole process was automated with MATLAB controlling the function calls and data manipulation. This allowed for simple experimentation as one element could be changed at a time and the effects easily seen.

5 SIMULATION RESULTS

The actual simulated experiment was to image an obscured object, and the following are results from the backscatter geometry. For comparison, two simulations were preformed, one with a wall obstruction and one without. The first description is of the geometry, with no obstruction, while the second is the same with the addition of an obstruction. The working geometry for the successful visible image reconstruction is as follows. A 5cm radius hollow aluminium sphere of thickness 0.8cm is centred at the origin. A conical x-ray source centred at (-100cm, 0) with an opening angle of 10° projected along the positive x-axis towards the sphere. The aperture is centred at (0, -40cm) extending 15.9cm in both the x and z direction. The detector is likewise centred at (0, -50cm) and extends 16cm in the x and z direction. There is lead shield protecting the detector from direct contributions from the source, which should not interfere with the backscatter.

The geometry of the second case, the obscured object remains the same with the addition of the wall. The important difference here is the addition of the wall which is made of 0.45cm thick pine, to simulate thin plywood. The wall begins centred at (0, 14cm) extending 50cm in both the x and y directions, directly in front of the aperture. It is then rotated 45° clockwise, so it conceals the object from the source and makes a 45° angle with both the source in the x direction and the aperture in y direction. With the exception of the light intensity difference, because the images are normalized to themselves, both sets of reconstructed images are very similar, to the effect that the object could be considered equally visible in either image.

The backscatter geometry with pine wall obstruction is shown in Figures 6, 7, 8 and 9:

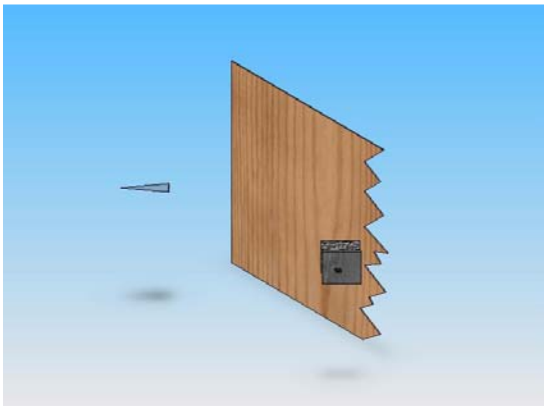

Figure 6: Isometric View

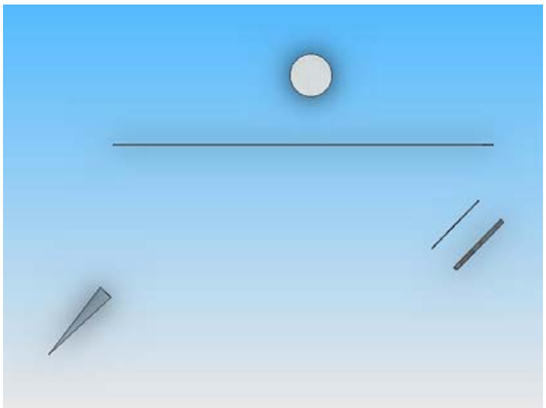

Figure 7: Top view

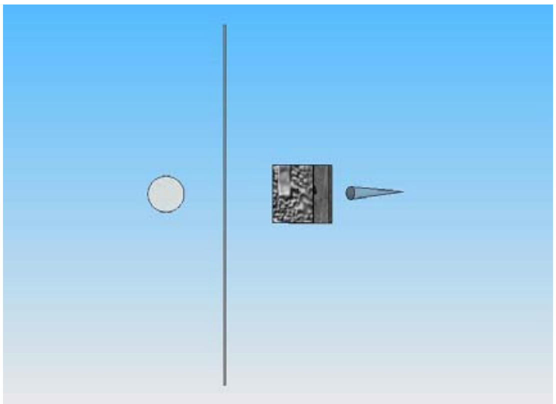

Figure 8: Left View

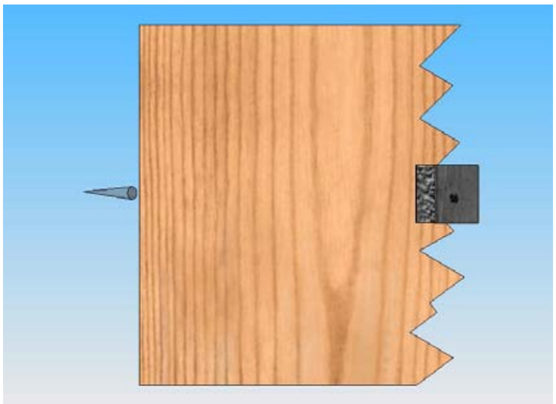

Figure 9: Front View

The results of the image reconstruction process are shown in Figure 10:

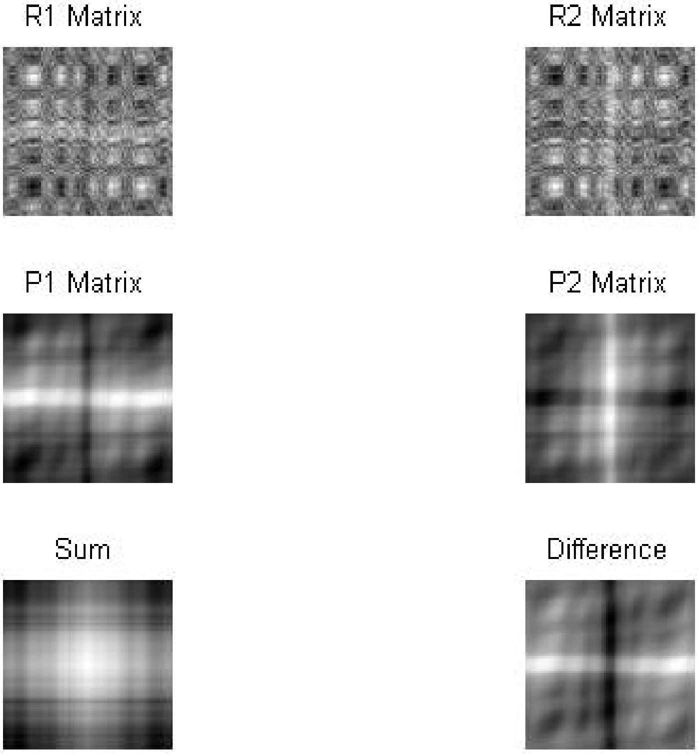

Figure 10: Image reconstruction of obscured sphere

Where R1 is the detector response for the mask, R2 is the detector response for the anti-mask, P1 is the reconstruction of R1, and P2 is the reconstruction of R2. The sum is P1 + P2 and difference is P1 - P2. Figure 11 represents the sum of the reconstructions for the case with no wall, while Figure 12 is the case with a pine wall obstruction.

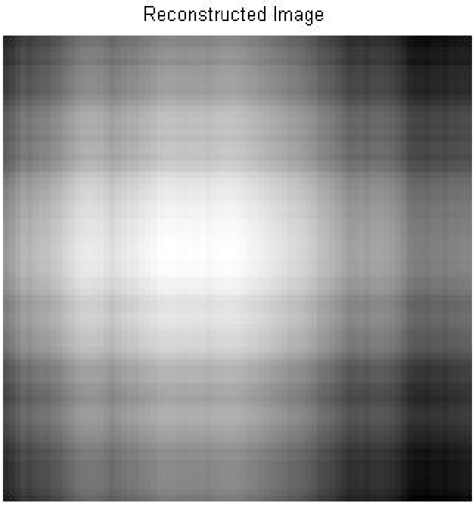

Figure 11: Sphere with no wall

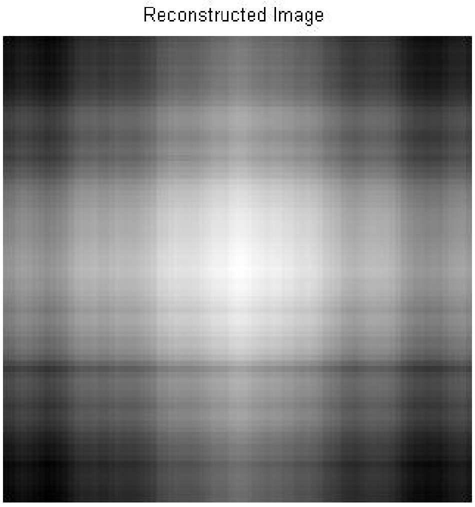

Figure 12: Sphere with pine wall

Pine was selected for the obstructing material, as it is a common building material in Canada. It's thickness was to approximate a common sheet of plywood. The source energy was chosen to be 10 MeV, an arbitrary value which can be easily modified in experiments. Simulations were conducted in a vacuum, with no scattering from air particles. The partial attenuation through the aperture and shield were removed, in that if a particle came into contact with the tungsten part of the aperture, it was ignored. In reality there is a small fraction of particles which will pass thought the solid aperture creating unwanted noise.

6 SUMMARY

Initially, a literature survey was conducted to gain an understanding of the available techniques used in one-sided imaging. From this, it was determined that the best choice for our research, in terms of simplicity regarding mask fabrication and decoding mathematics, was CAI. After reading published papers which discussed the mathematics, some basic apertures were simulated and simple objects successfully reconstructed in transmission mode, similar to a medical x-ray. This is the very basic geometry where the photons travel in a linear path from source to detector. The backscatter simulation, being more complex, showed some encouraging results, but will still require more time to develop fully.

The angle of most probable scatter was taken to be 45°, where the source and the detector were at right angles to each other. The optimal angle may be different than this, which might be discovered with an array of point detectors. Another possibility is that the angle must be varied in order to resolve edges in the image. This could mean fixing the source and detector on a plane and moving the plane closer or farther from the wall, or moving one of the two while the other remains still.

The simulated materials were chosen for their scattering properties, as a first estimate. This system could be calibrated better if there was a target in mind, such as humans or types of metal. In this manner, the scattering and source energy could be tuned to match the materials.

The current aperture size is 79 for ease of calculation. There are many other sizes which possess ideal imaging properties, documented in other research papers [1, 5, 10].

Research to date has been simulated on the computer; there is no guarantee that the real apparatus will behave the same way. For this reason, there will be some modifications to the simulated process to enable the imaging with our lab equipment. The results of the initial simulation indicate the feasibility of future imaging capabilities exceeding expectations.

7 CONCLUSION

The principle of coded apertures shows potential to image obscured objects because of its unique behaviour. The three challenges of CAI are aperture design, gamma ray detection and decoding procedures. The advantage is that one can choose each of the above three to any desired specifications. Since the object in focus will be considered “unmovable” the imaging system must operate independently of it. In this way, the three controls are within the operator’s power to change. The ability to use gamma and x-ray radiation as the imaging source, along with the unique properties of coded apertures give them the potential to be very useful in detecting visually obscured objects, providing the necessary tools are present to understand what is produced. The process of decoding and reconstructing the image will be done by a computer, without the need for a trained operator. This means when the technology is perfected, it can be applied to a wide range of applications. The only requirement at this point is a better understanding of the behaviour of coded apertures and how to best make use of this. The next phase of this research project will include improving the Monte Carlo backscatter simulations, simulating lower energy photon transport (down to 150 keV), fabricating a number of masks and performing experiments using an x-ray imaging system.

ACKNOWLEDGEMENTS

This research was conducted under the supervision of Dr. Edward Waller with funding provided by the University of Ontario Institute of Technology Faculty of Energy Systems and Nuclear Science.

REFERENCES

[1] Accorsi R. et al., “A Coded Aperture for High-Resolution Nuclear Medicine Planar Imaging with a Conventional Anger Camera: Experimental Results.” IEEE Trans. 2002. pp. 1587-1591.

[2] Gottesman, Stephen R., Fenimore E. E. New family of binary arrays for coded aperture imaging. Applied Optics. Vol 28. No 20. October 15 1989. pp. 4344-4352.

[3] Faust, A., “Detection of Explosive Devices Using X-ray Backscatter Radiation,” Canadian Patent 2 427 463, Oct. 30, 2004.

[4] Weisstein, Eric W. “Quadratic Residue.” Mathworld. June, 2005 http://mathworld.wolfram.com/QuadraticResidue.html

[5] Busboom, A. et al. Uniformly Redundant Arrays. Experimental Astronomy 8: 97-123, 1998.

[6] Pelowitz, Denise B. MCNPX User’s Manual Version 2.5.0. April 2005.

[7] MATLAB. The Mathworks. May, 2005. http://www.mathworks.com/access/helpdesk/help/techdocs/matlab.html

[8] Lanza et al., “Coded Aperture Imaging,” U.S. Patent 6,737,652, May 18, 2004.

[9] Zhang L. et al., “Pattern Design and Imaging Methods in 3-D Coded Aperture Techniques”, IEEE Trans. on Nucl. Sci., 1999 pp. 1521.

[10] McConnell, M. et al. “A Balloon-Borne Coded Aperture Telescope for Arc-Minute Angular Resolution at Hard X-Ray Energies”, Proc. SPIE Conf. 2806, 349, 1996.